ARTICLE

Quasiclassical Trajectory Study of the Reaction of CD_4 with $O(^1D)$[†]

Ke-jie Shao, Bi-na Fu[*], Dong H. Zhang[*]

State Key Laboratory of Molecular Reaction Dynamics and Center for Theoretical and Computational Chemistry, Dalian Institute of Chemical Physics, Chinese Academy of Sciences, Dalian 116023, China

(Dated: Received on July 15, 2015; Accepted on July 23, 2015)

Extensive quasiclassical trajectory calculations for the $O(^1D)+CD_4$ multichannel reaction were carried out on a new global potential energy surface fit by permutationally invariant polynomials. The product branching ratios, translational energy distributions, and angular distributions of $OD+CD_3$, $D+CD_2OD/CD_3O$, and D_2+DCOD/D_2CO product channels were calculated and compared with the available experimental results. Good agreement between theory and experiment has been achieved, indicating small isotope effects for the title reaction. The $O(^1D)+CD_4$ reaction mainly proceeds through the CD_3OD intermediate via the trapped abstraction mechanism, with initial abstraction of the D atom rather than the direct insertion, followed by decomposition of CD_3OD into various products.

Key words: Multichannel reaction, Reaction dynamics, Quasiclassical trajectory, Potential energy surface

I. INTRODUCTION

Methane is the simplest alkane and the most abundant hydrocarbon in the atmosphere. Extensive studies have been carried out in the past decades for methane reactions both experimentally and theoretically [1–12]. The reactions of $H+CH_4$, $F+CH_4$, $Cl+CH_4$, and $O(^3P)+CH_4$, known as the direct abstraction or exchange reactions, have been well studied and mostly understood now [1–12]. Another well-known class of reactions is the complex-forming reaction, in which a reaction intermediate exists. Such an intermediate is formed because of a potential well along the reaction path, and it eventually breaks apart to form the product species. Different from the reaction of ground state oxygen $O(^3P)$ with methane, the reactions of $O(^1D)$ with methane or other gas-phase molecules like NH_3, CH_4, C_2H_6 exhibit more complicated dynamical behaviors [13–18]. A deep well, which corresponds to the formation of intermediate complex, exits in these ground state potential energy surfaces (PESs). In addition, the character of multiple product channels in these reactions leads to the complexity of experimental and theoretical investigations.

The reaction of $O(^1D)$ with methane was long regarded as the prototype of polyatomic insertion reaction. Extensive experimental and theoretical studies have been carried out in order to get a detailed description of dynamics in this reaction system [14, 15, 19–30]. Theoretically, González *et al.* constructed an triatomic analytical ground state PES with methyl group treated as an atom by a many body expansion [27], based on low level of *ab initio* calculations. The trajectories of $O(^1D)+CH_4\rightarrow OH+CH_3$ show that the reaction takes place through the insertion reaction mechanism and can be divided into the direct or nondirect process with about the same probability. Yu and Muckerman characterized the ground state potential energy surface for $O(^1D)+CH_4$, and a direct-dynamics study of this reaction was performed [28]. However, due to the large computational effort this approach was entailed, a low-level electronic structure method was used and limited trajectories were propagated for a short time. A clear dynamical picture for the ground-state reaction was not obtained.

Experimentally, Yang and co-workers investigated the $O(^1D)+CH_4/CD_4$ reaction by performing the universal crossed molecular beam experiment [14] in 2000. The relative branching ratios of OH, H, and H_2 formation channels were determined to be 77%, 18%, and 5%, respectively. The differential cross section (DCS) of the OH formation channel shows a predominant forward scattering peak and a relatively small backward scattering peak, which is probably not consistent with the direct insertion reaction picture with forward backward scattering symmetry [31, 32]. Quite different from the OH channel, the H formation channel exhibits a slightly higher backward scattering, and the DCS of the H_2 formation channel shows an isotropic angular distribution. Recently, Suzuki and co-workers performed crossed molecular beam ion imaging experiment for the $O(^1D)+CH_4\rightarrow OH+CH_3$ reaction and its isotopes [20–22]. They observed two distinctive reaction mechanisms, in which the supposed "insertion" reaction

[†]Dedicated to Professor Qing-shi Zhu on the occasion of his 70th birthday.

[*]Authors to whom correspondence should be addressed. E-mail: bina@dicp.ac.cn, zhangdh@dicp.ac.cn

on the ground-state PES shows a dominantly forward scattering angular distribution, whereas the abstraction channel demonstrates obviously a backward scattering angular distribution with discrete structures and takes place much probably on the excited-state PES, as predicted by Hernando *et al.* [25]. More recently, a time-sliced velocity map imaging crossed beams experiment on the $O(^1D)+CD_4 \rightarrow OD+CD_3$ reaction was carried out by Yang and co-workers, indicating that the abstraction pathway is a minor process [23, 24], in accordance with the experimental results by Suzuki [21].

Although extensive studies have been carried out for the title reaction system, some detailed dynamics features remain unclear. A comprehensive theoretical investigation, which can explain the experimental results well, is still necessary. Very recently, we have newly constructed a full-dimensional ground-state PES for the $O(^1D)$ reaction with methane, based on high-level *ab initio* calculations. The detailed dynamics of the $O(^1D)+CHD_3 \rightarrow OH+CD_3$ reaction was investigated using quassiclassical trajectory (QCT) method on the new PES, together with the time-sliced ion velocity imaging crossed molecular beam experiment [30]. Very good agreement between theoretical and experimental results has been achieved. A new mechanism we termed "trapped abstraction" was uncovered by this study, demonstrating the initial abstraction of the H atom by $O(^1D)$ from CHD_3. The formation of extremely short-lived CD_3OH complex results in the dominantly forward scattering angular distribution [30].

In this work, we carried out the QCT studies of the $O(^1D)+CD_4$ multichannel reaction on the new PES, focusing not only on the OD formation channel, but also the D and D_2 formation channels. The calculated results were compared with those of the previously universal crossed molecular beam experiment when possible [14].

II. POTENTIAL ENERGY SURFACE AND QUASICLASSICAL TRAJECTORY CALCULATIONS

We developed a ground-state PES for the reaction of $O(^1D)$ and methane [30], using the permutationally invariant polynomial fitting procedure [33, 34]. A total of roughly 240,000 MRCI(Q)/aug-cc-pVTZ electronic energies were calculated by MOLPRO [35]. The orbitals for the MRCI(Q) calculations were taken from six-state complete-active-space self-consistent field (CASSCF) calculations using the dynamical weighting for each state. The active space used in both the CASSCF and MRCI(Q) calculations was 18 electrons in 10 orbitals and was chosen because it gave a consistent description of the wave function across the large regions of the PES of interest. The configurations used in the fitting were selected properly based on direct dynamics simulations and further QCT calculations using the preliminary PESs [36, 37]. Specifically, the initial data set consists of roughly 4×10^4 electronic energies with the configurations taken from direct dynamics calculations using the unrestricted B3LYP/6-31+G* method. For these calculations, a total of about 400 trajectories were run from the reagents $O(^1D)+CH_4$ at the collision energies of 6.8 and 10.0 kcal/mol, respectively. Additional ~400 trajectories were run initiated from the various transition state (TS) regions leading to different product channels. Starting from the first PES based on the initial ~40000 MRCI(Q)/aug-cc-pVTZ energies, more data points were added iteratively by doing QCT calculations on those preliminary PESs. The final fit includes all basis functions up to sixth order, for a total of 3262 coefficients. In the fit a configuration at energy E relative to the global minimum had weight $E_0/(E+E_0)$, where E_0=62 kcal/mol. The weighted RMS error of the fitted surface is 0.57 kcal/mol for energies up to 230 kcal/mol relative to the global minimum (methanol) of the PES. The final PES is well converged with respect to the fitting errors and dynamics features.

A complete schematic of the PES given in Fig.1 shows in detail the stationary point structures and energies relative to the reagents $O(^1D)+CD_4$ (with vibrational zero-point energies not included) corresponding to the relevant product channels. As seen, the CD_3OD molecule is located at −137.6 kcal/mol below the $O(^1D)+CD_4$ asymptote, indicating that the reaction can, in principle, evolve via this deep well on the PES and subsequently decompose to various products. Due to the complexity of the PES for this system, the fitting is challenging to describe accurately all of the stationary points and reaction channels. The comparisons made for the energies obtained from the current PES and MRCI(Q)/aug-cc-pVTZ calculations show good agreement among them. As seen in Fig.1, seven product channels OD+ CD_3, $D+CD_3OD/CD_2OD$, $D_2+D_2CO/$*trans*-DCOD/*cis*-DCOD, and D_2O+CD_2, might be formed in the $O(^1D)+CD_4$ multichannel reaction.

The QCT calculations were carried out at the experimental collision energy (E_c) of 6.8 kcal/mol from the reactants on the current PES with CD_4 in the ground rovibrational state. The quasiclassical ground vibrational state of CD_4 was set by randomly sampling the normal coordinates and momenta for zero angular momentum. Adjustments were then made to the momenta to enforce zero angular momentum of CD_4. The initial distance of the $O(^1D)$ atom from the center of mass of the CD_4 molecule was $\sqrt{x^2+b^2}$, where b was the impact parameter and x was set to be 11.0 bohrs. The orientation of CD_4 was randomly sampled with respect to the $O(^1D)$ atom, and b was selected randomly from the distribution $b_{\max}\sqrt{r}$, where r was a random number uniformly distributing from 0 to 1. The employed $b_{\max}$ value was 7.0 bohr at E_c=6.8 kcal/mol. Roughly 7×10^6 trajectories were run using velocity verlet integration algorithm with a step size of 0.12 fs for a maximum time of 10 ps. The ZPE constraint results [37–39], obtained from those trajectories in which each product has at

DOI:10.1063/1674-0068/28/cjcp1507152

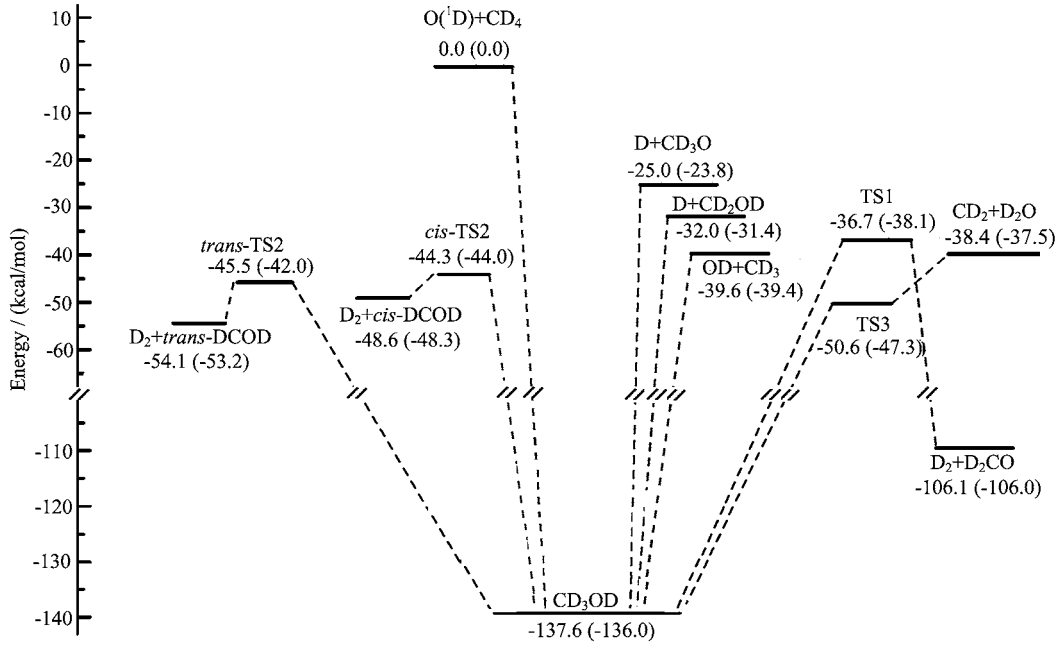

FIG. 1 Schematic of the ground-state PES of the $O(^1D)+CD_4$ multichannel reaction. The fitted energies are in kcal/mol, relative to the reactants $O(^1D)+CD_4$, and those shown in parentheses are from MRCI+Q/aug-cc-pVTZ calculations. All of the energies are shown without vibrational zero-point energy correction.

least the corresponding ZPE are given in this study.

III. DYNAMICS RESULTS

A. Branching ratios of different reaction pathways

The relative branching ratios for the $O(^1D)+CD_4$ reaction at E_c=6.8 kcal/mol were determined by current theory:

$$\begin{aligned}
O(^1D) + CD_4 &\rightarrow OD + CD_3 && (71.6\%)\ (1)\\
&\rightarrow D + CD_2OD && (14.2\%)\ (2)\\
&\rightarrow D + CD_3O && (3.1\%)\ (3)\\
&\rightarrow D_2 + D_2CO && (1.3\%)\ (4)\\
&\rightarrow D_2 + trans\text{-DCOD} && (2.2\%)\ (5)\\
&\rightarrow D_2 + cis\text{-DCOD} && (1.3\%)\ (6)\\
&\rightarrow D_2O + CD_2 && (6.3\%)\ (7)
\end{aligned}$$

The primary product branching ratios for the $O(^1D)+CH_4$ reaction were measured by Yang and coworkers [14]. However, the water product channel can not be detected due to the low experimental resolution at that time. Therefore, the D_2O+CD_2 channel is not included in the accounting of the percentages from theory to be compared with the experiment. The branching ratios of OD ($OD+CD_3$), D ($D+CD_2OD$ and $D+CD_3O$), and D_2 (D+DCOD and D_2CO) formation channels obtained by the QCT calculations are 76.4%, 18.5%, and 5.1%, in very good agreement with the experimental results of 77%, 18%, and 5% for OH ($OH+CH_3$), H ($H+CH_2OH$ and CH_3O), and H_2 (H_2+HCOH and H_2CO) channels, respectively. This suggests small isotope effects for the title reaction.

B. OD formation channel

As shown above, $OD+CD_3$ is the main product channel of the $O(^1D)+CD_4$ reaction. The angular distribution of CD_3 and translational energy distribution of $OD+CD_3$ obtained by the QCT calculations are shown in Fig.2. The angular distribution of the OD product shows a pronounced forward scattering peak relative to the $O(^1D)$ beam direction, with a relatively small backward scattering peak and small signals from the sideways scattering. The behavior of this distribution closely resembles the experimental results of $O(^1D)+CH_4\rightarrow OH+CH_3$ by Yang and co-workers [14], although the direct abstraction reaction occurs on the excited-state PES, which can also form backward scattering products, is ignored in the current theory due to its small contributions to the overall reactivity. This dynamical picture is not consistent with the direct insertion reaction as has long been thought, which probably leads to the forward and backward scattering symmetry. Very recently, a new reaction mechanism we termed "trapped abstraction" for the $O(^1D)+CHD_3\rightarrow OH+CD_3$ reaction is unraveled by us [30]. We found that the $O(^1D)+CD_4\rightarrow OD+CD_3$ reaction mainly proceeds via this new mechanism as well, but not the direction insertion. The $O(^1D)$ initially abstracts the D atom out of CD_4, rather than inserting into the C−D bond, followed by the formation of the

DOI:10.1063/1674-0068/28/cjcp1507152

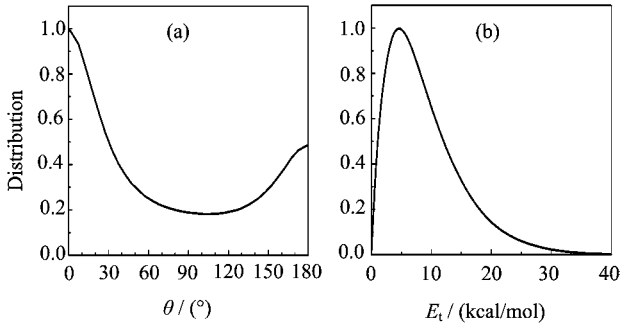

FIG. 2 (a) Scattering angular (θ) distribution of OD relative to the direction of the incoming O(^{1}D). (b) Translational energy (E_t) distribution of OD+CD_3 obtained from the QCT calculations.

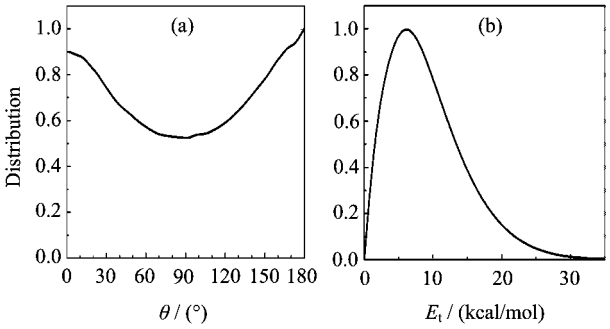

FIG. 3 (a) Scattering angular (θ) distribution of CD_2OD/CD_3O relative to the direction of the incoming O(^{1}D). (b) Total translational energy (E_t) distribution of the D formation channel (D+CD_2OD and D+CD_3O).

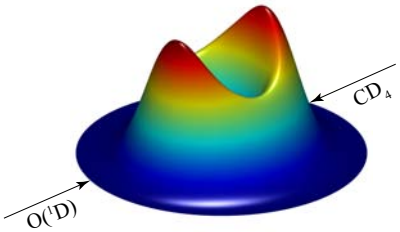

FIG. 4 3D polar plot for the product translational energy and angular distributions for the D formation channel. The forward direction (0°) corresponds to the direction of the O(^{1}D) reagent.

CD_3OD intermediate. The process with a short lifetime behaves like an abstraction reaction, producing a pronounced forward scattering peak by a stripping mechanism with large impact parameter, while the process with a long lifetime produces reaction products with forward and backward scattering symmetry, similar to an insertion reaction. Hence, we observed dual characters of an abstraction reaction and an insertion reaction in the O(^{1}D)+CD_4→OD+CD_3 reaction pathway.

As shown in Fig.2(b), the behavior of the translational energy distribution supports that the pathway leading to CD_3+OD on the ground-state PES is barrierless. This distribution is narrow peaked at around 5.0 kcal/mol, with a long tail up to the energy of roughly 37.0 kcal/mol. The averaged translational energy release for this channel is small, indicating that most of the available energy in this channel is deposited into the internal degrees of freedom of the molecular radical products, in accordance with the experimental measurement for the O(^{1}D)+CH_4→OH+CH_3 reaction channel [14].

C. D formation channel

There are two D atom formation pathways, D+CD_2OD and D+CD_3O, on the ground-state PES of the title reaction, as shown in Fig.1. As discussed above, the relative branching ratio of D+CD_2OD is about 4 times larger than that of D+CD_3O, indicating D+CD_2OD is the dominant product for the D formation channel. Due to the similar behavior of product angular and translational energy distributions between the two D formation channels obtained in the QCT calculations, we display the total angular and translational energy distributions of the two channels in Fig.3. We can see from Fig.3(a) that the CD_2OD/CD_3O product is slightly backward scattered, nearly symmetric with respect to the forward and backward directions, as expected for a long-time complex formation reaction. This overall behavior is in accordance with the experimental results for the D formation channel in the O(^{1}D)+CD_4 reaction [14], except that a more obvious backward scattering peak was observed in the experiment. The translational energy distribution shown in Fig.3(b) peaks at about 7 kcal/mol and vanishes at the energy of about 32 kcal/mol. The small fraction of energy in translation indicates most of the available energy is channeled into the internal excitations of CD_2OD/CD_3O. The overall behavior of the translational energy distribution is quite similar to that of the experimental results [14], which supports that the dynamics of this channel is barrierless.

Figure 4 shows a 3D polar plot for the product translational energy and angular distributions for the D formation channel. As seen, the forward and backward scattering signals are stronger than those of the sideways scattering. In the experimental 3D polar plot, the product looks slightly backward scattered, which resembles that of the theoretical results showing more forward and backward scattering symmetry. Further analysis of the trajectories shows that the D formation pathway mainly proceeds through the CD_3OD intermediate, starting with the abstraction of the D atom, similar to the initial step in producing OD+CD_3. A tiny portion (<1%) of trajectories goes through the typical direct insertion pathway, with the O(^{1}D) atom directly inserting into the C−D bond of CD_3. Nonetheless, only the CD_3OD intermediate with a long lifetime produces D+CD_2OD/CD_3O, leading to the almost forward and

DOI:10.1063/1674-0068/28/cjcp1507152

backward scattering symmetry, similar to an insertion reaction.

D. D_2 formation channel

As shown in Fig.1, there are three D_2 formation pathways on the ground-state PES via the CD_3OD intermediate, which decomposes to D_2+*cis*-DCOD, D_2+*trans*-DCOD and D_2+D_2CO, respectively. The relative fraction of D_2+DCOD (the sum of *cis*-DCOD and *trans*-DCOD) versus D_2+D_2CO is roughly 3:1 obtained from the current theory. The D_2CO channel is less favorable, due to a much higher reverse barrier than the DCOD process.

Figure 5(a) shows the total angular distribution of the D_2 formation channel. We can see the nearly isotropic angular distribution of the D_2 formation channel, with slight preference for the forward scattering and backward scattering. By investigating the trajectories for the two channels, we find a long-lived intermediate CD_3OD is formed before its decomposition, similar to the D formation channel. In addition, the complex is nearly exclusively formed by the abstraction of D atom from CD_4 by $O(^1D)$, followed by sliding into the deep CD_3OD well, but not by the direction insertion of $O(^1D)$ into the C−D bond of CD_4.

The total translational energy distribution of the D_2 formation channel is shown in Fig.5(b). Interestingly, the translational energy distribution displays a clear bimodal structure, with one peak at around 20 kcal/mol and one at roughly 60 kcal/mol, in good accordance with the experimental results [14]. As shown in Fig.1, the *cis*-DCOD and *trans*-DCOD channels are produced via the similar barrier heights (differing by ∼1 kcal/mol) starting from CD_3OD, with the reaction exothermicity differing by ∼5 kcal/mol, while the D_2CO channel is formed through a higher barrier and with much more exothermicity. As D_2+DCOD and D_2+D_2CO formation pathways are energetically significantly different from each other, the D_2+D_2CO channel produces the higher translational energy peak and the D_2+DCOD channel leads to a lower peak, which has a much lower reverse reaction barrier. The overall behavior of the translational energy distribution supports that the dynamics of the two channels is dominated by the exit channel barrier, which is quite different from that of D+CD_2OD/CD_3O or OD+CD_3.

The 3D polar plot for the translational energy distribution and angular distribution of the D_2 formation channel is depicted in Fig.6. Since the reaction exothermicity and translational energy distributions are quite different for the D_2CO and DCOD channels, the outer-sphere distribution with larger velocity arises from the D_2CO channel, and the inner-sphere distribution with smaller velocity results from the DCOD channel. Both the two D formation channels yield products with isotropic angular distributions.

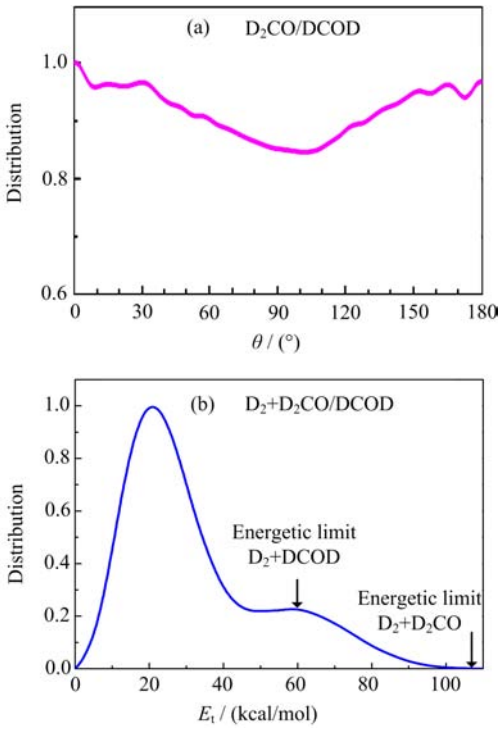

FIG. 5 (a) Scattering angular (θ) distribution of DCOD/D_2CO relative to the direction of the incoming $O(^1D)$. (b) Total translational energy (E_t) distribution of the D_2 formation channel. The total available energies for D_2+DCOD and D_2+D_2CO channels are indicated by arrows, respectively.

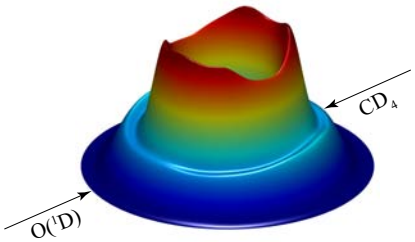

FIG. 6 3D polar plot for the product translational energy and angular distributions for the D_2 formation channel. The forward direction (0°) corresponds to the direction of the $O(^1D)$ reagent.

IV. CONCLUSION

To summarize, extensive QCT calculations for the $O(^1D)$+CD_4 reaction have been carried out on a new full-dimensional PES fit to MRCI+Q/aug-cc-pVTZ energies by permutationnaly invariant polynomials. The detailed dynamics information of OD+CD_3, D+CD_2OD/CD_3O and D_2+DCOD/D_2CO product channels were investigated and compared with the available experimental results. The primary product branching ratios, translational energy and angular distributions from the current theory are in accordance with the previous experimental results.

DOI:10.1063/1674-0068/28/cjcp1507152

Detailed analysis indicates the $O(^1D)+CD_4$ multichannel reaction mainly proceeds through the CD_3OD intermediate via the trapped abstraction mechanism [30], starting with the abstraction of the D atom from CD_4 by $O(^1D)$, with only a tiny portion of trajectories going through the typical direct insertion pathway. The trajectories with short lifetimes behave as an abstraction reaction and thus result in the dominantly forward scattering of the $OD+CD_3$ reaction pathway. A large portion of trajectories are trapped in the CD_3OD well for long time, although they also start with the abstraction of the D atom. These kinds of trajectories manifest as those for an insertion barrierless reaction, producing products with nearly forward and backward symmetry, as found in all the reactive trajectories of the D formation channel and some reactive trajectories of the OD channel. The reaction mechanism of the D_2 formation channel is similar to the D formation channel, except that the former is dominated by the exit channel barrier. We anticipate that the trapped abstraction mechanism should also be responsible for the reaction of $O(^1D)$ with ethane and propane, as well as many other chemical reactions with deep wells in the interaction region.

V. ACKNOWLEDGMENTS

This work was supported by the National Natural Science Foundation of China (No.21303197 and No.90921014), the Ministry of Science and Technology of China (No.2013CB834601), and Chinese Academy of Sciences.

[1] Y. Zhou, B. Fu, C. Wang, M. A. Collins, and D. H. Zhang, J. Chem. Phys. **134**, 064323 (2011).
[2] R. Welsch and U. Manthe, J. Chem. Phys. **141**, 051102 (2014).
[3] J. J. Lin, J. Zhou, W. Shiu, and K. Liu, Science **300**, 966 (2003).
[4] J. P. Camden, H. A. Bechtel, D. J. Ankeny Brown, M. R. Martin, R. N. Zare, W. Hu, G. Lendvay, D. Troy, and G. C. Schatz, J. Am. Chem. Soc. **127**, 11898 (2005).
[5] S. Yan, Y. T. Wu, B. Zhang, X. F. Yue, and K. Liu, Science **316**, 1723 (2007).
[6] W. Zhang, H. Kawamata, and K. Liu, Science **50**, 303 (2009).
[7] W. Zhang, Y. Zhou, G. Wu, Y. Lu, H. Pan, B. Fu, Q. Shuai, L. Liu, S. Liu, L. L. Zhang, B. Jiang, D. Dai, S. Y. Lee, Z. Xie, B. J. Braams, J. M. Bowman, M. A. Collins, D. H. Zhang, and X. Yang, Proc. Natl. Acad. Sci. USA **107**, 12782 (2010).
[8] G. Czakó, and J. M. Bowman, Science **334**, 343 (2011).
[9] G. Czakó and J. M. Bowman, Proc. Natl. Acad. Sci. USA **109**, 7997 (2012),
[10] Z. Zhang, Y. Zhou, D. H. Zhang, G. Czakó, and J. M. Bowman, J. Phys. Chem. Lett. **3**, 3416 (2012).
[11] R. Liu, M. Yang, G. Czakó, J. M. Bowman, J. Li, and H. Guo, J. Phys. Chem. Lett. **3**, 3776 (2012).
[12] R. Welsch and U. Manthe, J. Phys. Chem. Lett. **6**, 338 (2015).
[13] J. Shu, J. J. Lin, C. C. Wang, L. Y. T. Lee, and X. Yang, J. Chem. Phys. **115**, 842 (2001).
[14] J. J. Liu, J. Shu, Y. T. Lee, and X. Yang, J. Chem. Phys. **113**, 5287 (2000).
[15] X. Yang, Phys. Chem. Chem. Phys. **8**, 205 (2006).
[16] J. Shu, J. J. Lin, Y. T. Lee, and X. Yang, J. Chem. Phys. **115**, 849 (2001).
[17] J. Shu, J. J. Lin, Y. T. Lee, and X. Yang, J. Chem. Phys. **114**, 4 (2001).
[18] J. Shu, J. J. Lin, Y. T. Lee, and X. Yang, J. Am. Chem. Soc. **123**, 322 (2001).
[19] C. C. Miller, R. van Zee, and J. Stephenson, J. Chem. Phys. **113**, 5287 (2000).
[20] H. Kohguchi, Y. Ogi, and T. Suzuki, Phys. Chem. Chem. Phys. **10**, 7222 (2008).
[21] H. Kohguchi, Y. Ogi, and T. Suzuki, Phys. Chem. Chem. Phys. **13**, 8371 (2011).
[22] Y. Ogi, H. Kohguchi, and T. Suzuki, Phys. Chem. Chem. Phys. **15**, 12946 (2013).
[23] Q. Shuai, H. Pan, J. Yang, D. Zhang, B. Jiang, D. Dai, and X. Yang, J. Phys. Chem. Lett. **3**, 1310 (2012).
[24] Q. Shuai, H. Pan, J. Yang, D. Zhang, B. Jiang, D. Dai, and X. Yang, J. Chem. Phys. **137**, 224301 (2012).
[25] J. Hernando, J. Millán, R. Sayós, and M. González, J. Chem. Phys. **119**, 9504 (2003).
[26] R. Sayós, J. Hernando, M. P. Puyuelo, P. A. Enriquez, and M. González, Phys. Chem. Chem. Phys. **4**, 288 (2002).
[27] M. González, J. Hernando, I. Baños, and R. Sayós, J. Chem. Phys. **111**, 8913 (1999).
[28] H. G. Yu and J. T. Muckerman, J. Phys. Chem. A **108**, 8615 (2004).
[29] R. B. Bouchrit, M. Jorfi, D. B. Abdallah, N. Jaidane, M. González, B. Bussery-Honvault, and P. Honvault, J. Chem. Phys. **140**, 244315 (2014).
[30] J. Y. Yang, K. J. Shao, D. Zhang, Q. Shuai, B. Fu, D. H. Zhang, and X. Yang, J. Phys. Chem. Lett. **5**, 3106 (2014).
[31] X. Liu, J. J. Lin, S. Harich, G. C. Schatz, and X. Yang, Science **289**, 1536 (2000).
[32] H. Guo, Int. Rev. Phys. Chem. **31**, 1 (2012).
[33] B. J. Braams and J. M. Bowman, Int. Rev. Phys. Chem. **28**, 577 (2009).
[34] J. M. Bowman, G. Czakó, and B. Fu, Phys. Chem. Chem. Phys. **13**, 8094 (2011).
[35] H. J. Werner and P. J. Knowles, *MOLPRO, version 2010.1*, *A Package of ab initio Programs*, http://www.molpro.net/, (2010).
[36] Y. Han, B. C. Shepler, and J. M. Bowman, J. Phys. Chem. Lett. **2**, 1715 (2011).
[37] B. Fu, D. H. Zhang, and J. M. Bowman, J. Chem. Phys. **139**, 024303 (2013).
[38] B. Fu, Y. Han, J. M. Bowman, L. Angelucci, N. Balucani, F. Leonori, and P. Casavecchia, Proc. Natl. Acad. Sci. USA **109**, 9733 (2012).
[39] B. Fu, Y. Han, J. M. Bowman, F. Leonori, N. Balucani, L. Angelucci, A. Occhiogrosso, R. Petrucci, and P. Casavecchia, J. Chem. Phys. **137**, 22A532 (2012).

DOI:10.1063/1674-0068/28/cjcp1507152